LAWRENCE
LIVERMORE
NATIONAL
LABORATORY

UCRL-JRNL-210340

Evaluation of a novel UHMWPE bearing for applications in precision slideways

E. S. Buice, H. Yang, S. T. Smith, R. J. Hocken, R. M. Seugling

March 9, 2005

Precision Engineering

Evaluation of a novel UHMWPE bearing for applications in precision slideways

Eric S. Buice [a,*], Hua Yang [a], Stuart T. Smith [a], Robert J. Hocken [a] and Richard M. Seugling [b]

[a] *University of North Carolina at Charlotte, Charlotte, NC 28223, USA*
[b] *Lawrence Livermore National Laboratory, Livermore, CA 94551, USA*

Abstract

This paper presents a novel slideway bearing design comprised of a thin-film (0.1 mm – 0.2 mm) of ultra-high molecular weight polyethylene (UHMWPE) bound to a rigid hemispherical substrate. Two prototype bearing designs were fabricated and tested to characterize the coefficient of friction (dynamic and static) and wear of the polymer. In addition, similar bearings were incorporated into a kinematically constrained rectilinear carriage to determine the repeatability of motion during multiple traverses. The first bearing had a radius of curvature on the order of 2.38 mm incorporating an UHMWPE film thickness between 0.1 mm and 0.2 mm. The friction coefficient was measured to be between 0.155 and 0.189 for normal loads of 11.5 N and 2.2 N, respectively at a surface speed of 4.2 $mm \cdot s^{-1}$. This bearing failed after a traverse of approximately 700 m at a load of 11.5 N. A similar evaluation procedure was carried out on a bearing of radius 6.35 mm resulting in a friction coefficient between 0.125 and 0.185 at loads of 27.8 N and 2.2 N, respectively, and the bearing endured a traverse of over 2.2 km at a load of approximately 28 N (in both air and vacuum conditions) with a surface speed of 4.2 $mm \cdot s^{-1}$. The second bearing prototype was further subjected to a repeatability test. In this setup, a carriage incorporating five bearings was traversed in a nominally linear path while vertical

* Corresponding author. Tel.: +1-704-687-3196; fax: +1-704-687-3246.
E-mail address: esbuice@uncc.edu (E.S. Buice)

deviations for multiple traverses were measured by a custom built displacement sensor. Deviations from a linear path were observed to repeat to within a few nanometers about nominal variations of less than 10 nm for a traverse distance of 10 mm. This system and other subsystems used to characterize the friction coefficient and noise of the polymer bearing are presented.

Keywords: UHMWPE, bearing design, precision slideways, wear, vacuum, friction coefficient.

1. Introduction

As machines and instruments continue to push for higher precision and accuracy, while maintaining a reasonable cost, it has become increasingly more important to find new methods to meet these requirements. The approach outlined in this paper is the use of thin-film (0.1 mm – 0.2 mm) ultra-high molecular weight polyethylene (UHMWPE) bearings. This bearing is a variant of the PTFE bearing utilized in ultra-precise machines such as the Nanosurf II [1], Nanosurf IV [2], and Tetraform [3] where sub-nanometer performance has been demonstrated. For relatively low loads and speeds, it is possible that the UHMWPE bearings will become an alternative to other contact and non-contact precision bearings. To achieve this, the new bearing design ought to be easily manufactured, low-cost, robust, vacuum compatible, and perform at sub-nanometer levels. In addition to the local pressure and velocity limitations, performance measures important for instrument bearing applications include heat removal at the interface, wear, stiffness, thermo-mechanical characteristics, accuracy of the datum counterface and frictional characteristics (in particular, stiction and load dependence) [4].

From previous research performed by Wang and Li [5], the friction coefficient of bulk UHMWPE sliding against ASTM 1045 steel was observed between 0.09 and 0.1 after an initial break-in period with dead weight loads ranging between 15 kg and 50 kg. Increasing the load and velocity on the UHMWPE, results in an apparent exponential increase of wear. This can best be described by three succinct phases: running-in, steady-state, and severe wear. Wang and Li further discussed a decrease in melting temperature between worn and unworn UHMWPE, which is believed to result from thermal softening of the surface layer of UHMWPE. It should be noted that the UHMWPE bearing described in this article will operate in an ultra-mild wear regime (speeds of up to 5 $mm \cdot s^{-1}$ and loads up to 28 N), while work performed from the above mentioned authors was typically performed to assess UHMWPE for artificial joint replacement where higher loads and speeds were in question. Considering the ultra-mild wear regime, Dowson, *et al*. has shown that UHMWPE under a load of 100 N at a surface speed of 0.25 $m \cdot s^{-1}$ had a wear factor between 18000 $mm^3 \cdot N^{-1} \cdot m^{-1}$ to 160000 $mm^3 \cdot N^{-1} \cdot m^{-1}$ against a counterface roughness of 13 nm [6].

2. UHMWPE Material Characteristics

UHMWPE was chosen for its desirable characteristics of low coefficient of friction and wear rate. Friction between a smooth counterface, such as an optical flat, and UHMWPE is primarily a function of adhesion, although other phenomena are most certainly involved. Typically, during the first few traverses, it has been observed that the friction coefficient be on the order of 0.2-0.3 then reducing to 0.15 after an initial break-in period [4]. It is believed that when UHMWPE is slid across a smooth counterface a layer of UHMWPE (a few to hundreds of nanometers in thickness) is deposited onto the counterface surface, while at the track end, a quantity of up to a 1.0 mm may be observed. The formed layer of

Table 1: Selected material properties of UHMWPE.

Material Property	UHMWPE
Coefficient of Expansion ($^oK^{-1}$)	200
Density ($kg{\cdot}m^{-3)}$	930
Dynamic friction coefficient	0.09 – 0.3
Heat capacity ($kJ{\cdot}(kg{\cdot}^oC)^{-1}$)	2
Maximum operating temperature (^oC)	77
Maximum pressure (MPa)	7
Poisson's ratio	0.46
Tensile strength (MPa)	41
Thermal conductivity ($W{\cdot}(m{\cdot}^oK)^{-1}$) @ 23 ^oC	0.42 – 0.51
Young's modulus (MPa)	689
Wear type	Adhesion

UHMWPE is believed to act as a self-lubricating mechanism, which results in a reduction of the coefficient of friction [7]. This concept is also in agreement with the observations of Unal, *et al*. [8]. The wear rate is also dependent on the surface roughness, where these rates can vary by a factor of 10 to 1000 with the presence of a few small, sharp cracks on the counterface [6]. UHMWPE has relatively weak intermolecular bonding with a high degree of crystallinity, which is the result of linear, branch-free molecular chains without any polar side groups. Table 1 shows selected bulk material properties for common UHMWPE [9, 10, 11].

3. Contact methodology

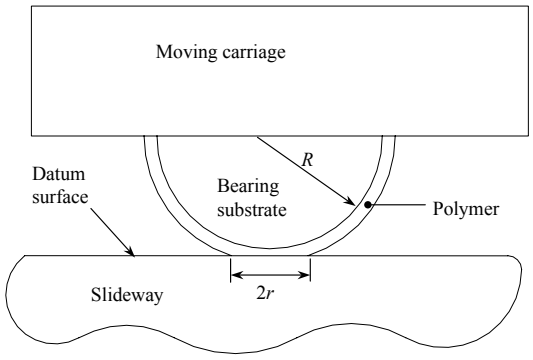

Fig. 1 Schematic representation of UHMWPE bearing.

The sliding friction or friction force of the bearing, shown schematically in Fig. 1, can be modeled by a combination of adhesion-shearing theory and a Winkler elastic foundation [12]. Following this approach, the friction force, F_f is considered to be a simple superposition of these two effects, thereby giving

$$F_f = F_s + F_d \tag{1}$$

where, F_s is the friction due to shearing, and F_d is the deformation resistance of the contact region. For a hertzian contact, the resistance to deformation is much smaller than that due to shearing, hence it may be assumed that (1) becomes

$$F_f = F_s = A\tau = \mu N \tag{2}$$

where, τ is the shear strength (or the adhesion constant) of the contact, A is the apparent contact area, μ is the coefficient of friction and N is the normal load. The apparent contact area can be calculated with the use of the Winkler elastic foundation (also known as the 'mattress') given by,

$$A = r^2\pi \,. \tag{3}$$

The contact radius, r is given by [13],

$$r = \left(\frac{4NRh}{\pi E^*}\right)^{1/4} \tag{4}$$

where, R is the radius of the sphere, h is the film thickness of UHMWPE, and E^* is the equivalent modulus of elasticity. E^* is defined as [14],

$$E^* = \left(\frac{1-\upsilon_1}{E_1} + \frac{1-\upsilon_2}{E_2}\right)^{-1} \tag{5}$$

where, E_1 and E_2 are the modulus of elasticity of each material and υ_1 and υ_2 are the Poisson's ratio of two different materials. Substituting (4) into (3) gives

$$A = \left(\frac{4\pi NRh}{E^*}\right)^{1/2} . \tag{6}$$

Solving for μ in (2) and substituting (6) gives

$$\mu = \tau\left(\frac{4\pi Rh}{NE^*}\right)^{1/2}. \tag{7}$$

Finally, substituting (5) into (7) gives

$$\mu = \tau\left(\frac{4\pi Rh\left(E_1 + E_2 - E_1\upsilon_2 - E_2\upsilon_1\right)}{NE_1E_2}\right)^{1/2}. \tag{8}$$

From (8) it is apparent that μ is an inverse function of the load N. Thus, as N is increased μ becomes smaller even though the friction force increases, see Fig. 2. The above formulation, while reflecting a trend observed in experiments, is based on the following assumptions

- Surface finish is ignored, which must be true for (6) to be satisfied
- τ is the shear strength of the interface between the polymer and counterface

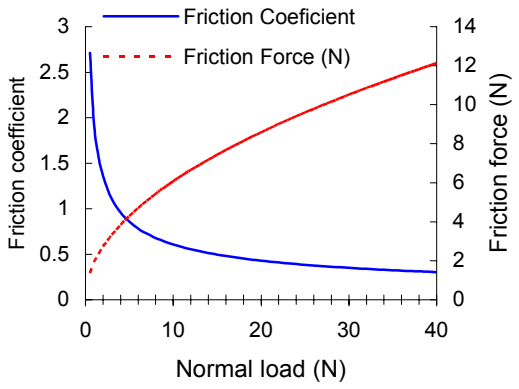

Fig. 2 Calculated friction coefficient and friction force as a function of normal load.

In principle, the shear strength could be calculated with the use of the Duprè equation in which the surface energy, representing the work required to separate the interface, is given by [13],

$$\gamma = \gamma_1 + \gamma_2 - \gamma_{12} \tag{9}$$

where, γ_1 and γ_2 are the surface energy of the two individual materials and γ_{12} is the surface energy of the contacting materials. In practice, the interface surface energy tends to be very environmentally sensitive and will be a function of any surface alterations during sliding. Fig. 2 is calculated based on the assumption that the shear strength of the interface is equal to the bulk shear strength of the

softer UHMWPE and for a radius of curvature of 6.35 mm and a film thickness of 0.1 mm. This figure represents an upper bound of both the friction coefficient and friction force based on the assumptions stated previously.

4. Bearing Design

Polymers typically have a low modulus of elasticity and a relatively high yield stress. This enables the polymer to elastically conform to the smooth counterface as load is increased thereby, enables the use of the Winkler elastic foundation or 'mattress' of the contact area, $A\ (=\pi r^2)$, given in equation (6). A schematic representation of the bearing design is shown in Fig. 1.

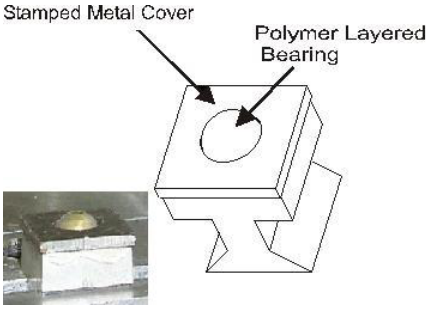

Fig. 3: First prototype bearing design with 2.38 mm radius of curvature.

In this article, two prototype bearings will be investigated. The first prototype bearing design utilized a brass substrate with a 2.38 mm radius of curvature, which is used to both support the thin polymer film and transfer the heat generated during sliding. To construct the bearing, thin-films of UHMWPE were skived from a solid piece of UHMWPE to a thickness between 0.1 mm and 0.2 mm. The polymer is then stretched over the brass sphere and held in place by a stamped sheet metal cover, see Fig. 3. This figure shows the fully assembled bearing design with overall dimension 9.5 mm × 9.5 mm × 11.6 mm. The second prototype bearing design, Fig. 4, was developed to provide better clamping of the polymer and enable a larger radius substrate surfaces to be generated. Increasing the radius of curvature to 6.35 mm theoretically provides an increase in contact area of nearly 60% and, correspondingly, a nearly 40% decrease in contact stress. To

achieve this radius, a 12.7 mm diameter sphere was turned in a lathe forming a cylinder with a diameter of 6 mm, while maintaining the 6.35 mm radius of curvature at both ends. The thin-film UHMWPE is then stretched over the brass cylinder and clamped in place in a mounting assembly, which can be secured into the slideway. The mounting assembly also features a height adjustment mechanism, via a setscrew from the back, to insure the slideway is sliding parallel to its counterface. The overall dimension of the second prototype bearing and mounting assembly is 25.4 mm × 38.1 mm × 12.7 mm.

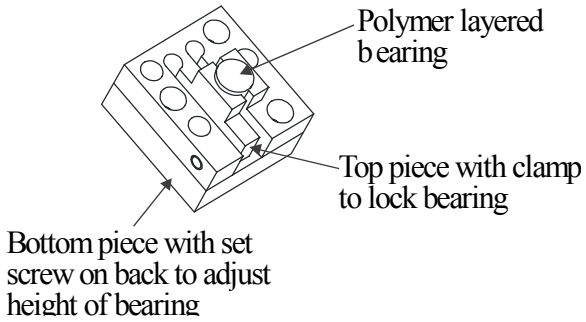

Fig. 4: Second prototype bearing design with 6.35 mm radius of curvature.

5. Test Equipment

To characterize the UHMWPE bearings two test instruments were designed and fabricated. The first test apparatus was based on the commonly used pin-on-disk apparatus to measure friction/stiction and evaluate the wear of the bearing at different surface speeds and normal loads. A second test apparatus constructed is a profilometer based instrument designed to measure the repeatability of the bearing moving along a nominally rectilinear trajectory.

5.1. Pin-on-Disk

To measure the coefficient of friction and evaluate wear a custom built pin-on-disk instrument was designed and is shown in Fig. 5. For the purpose of evaluating the performance of the bearings outlined in this paper, wear is defined as a perceptible reduction in volume of the bearing and/or counterface material resulting in degradation of

performance or catastrophic failure. This instrument has horizontal and vertical adjustments to position the bearing at a desired location on the rotating optical flat. The horizontal adjustment is used to set the sliding speed ranging from 2.1 $mm \cdot s^{-1}$ to 12.7 $mm \cdot s^{-1}$ by positioning the bearing radially from approximately 25 mm from the center to the edge of the optically flat, glass disk. The normal load is varied from 2.2 N to 28 N by adding dead weights to the horizontal moment arm. A flexure based load cell was developed to measure the lateral deflection of the bearing as it slides against the spinning disk. The load cell consists of a compliant flexure mechanism and a capacitive displacement sensor. Displacement was measured using a Lion Precision capacitance-based probe with a measurement range of ± 25.0 μm with an uncertainty of ± 4.7 nm.

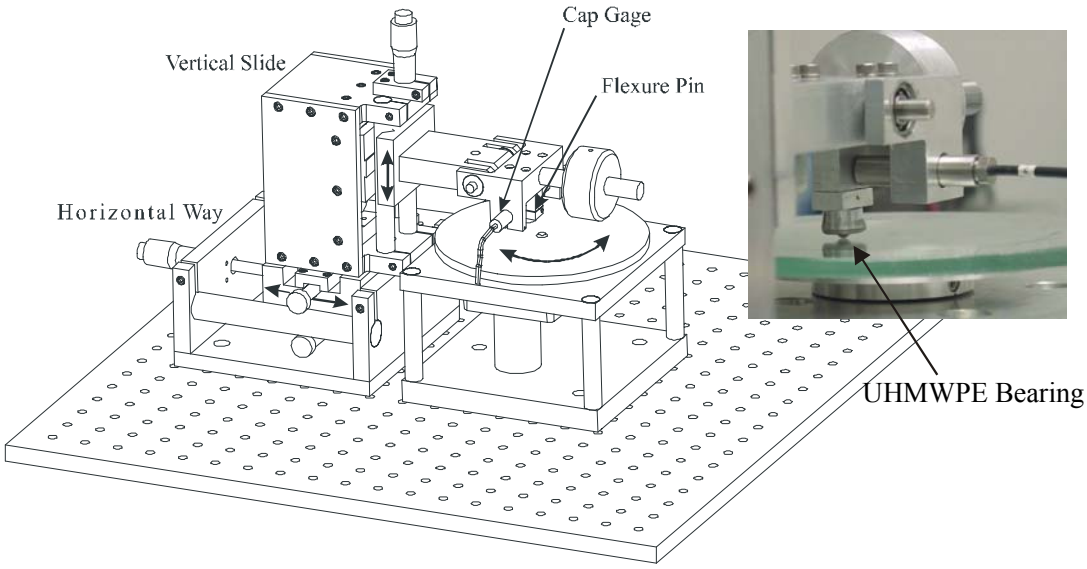

Fig. 5: Pin-on-disk test apparatus. Polymer bearing is rigidly fixed to the flexure pin as the glass counterface spins.

The friction coefficient of the polymer was computed with a known normal load and a calibrated frictional force. Calibration of the dead weight load was obtained from an Ohaus® precision balance and includes the mass contribution of the pivoting mechanism and the location of the mass on the moment arm. Additional dead weight can be added

directly above the polymer bearing to increase the load if desired. The flexure based load cell was calibrated by placing the pin-on-disk orthogonal to gravity, so that the rotating optical flat is in a vertical position. Dead weights were hung at the bearing mount coincident with gravity and the subsequent deflection of the sensor was measured by the displacement gage providing the force calibration data of sensor. This resulted in a sensitivity of 4.57 $V \cdot N^{-1}$ with a standard deviation of 0.23 $V \cdot N^{-1}$ (this is primarily due to uncertainty of load positioning during calibration).

5.2. Stylus Profilometer

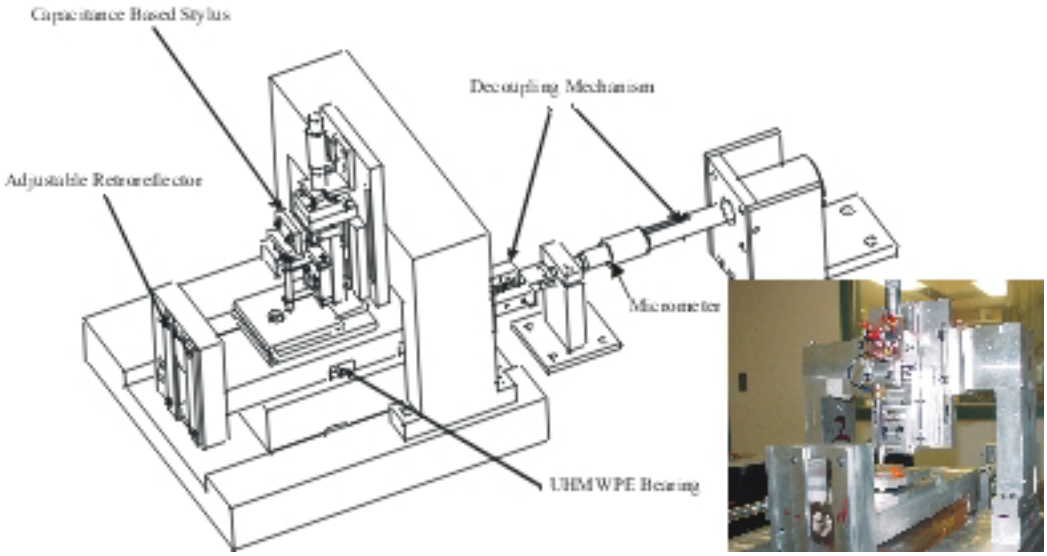

Fig. 6: Profilometer test fixture comprised of rectilinear slideway, capacitance based stylus probe, laser interferometer and drive motor.

To assess the repeatability and noise of the UHMWPE bearings, a stylus profilometer instrument was designed. The profilometer instrument incorporates a slideway with five kinematically positioned bearings contacting a rectangular optical flat that acts as a smooth, flat datum surface to produce a nominally rectilinear motion, as illustrated in Fig. 6. The bearing positions within the slideway are shown in Fig. 7. Contact between the bearings

and counterface was maintained by a combination of the mass of the stage and a decoupled preload mechanism. Translation of the slideway is achieved by decoupling a DC motor that is connected to the slideway through a non-rotating micrometer converting rotational motion to linear translation. To measure the vertical deviations of the slideway a stylus profiling sensor was constructed and used as a measure of the bearing repeatability. To provide a smooth, flat surface a 25.4 mm diameter optical flat was used as the artifact contacted by the stylus probe, while the linear translation of the slideway is monitored by an Optodyne™ laser interferometer. Clearly, measurement of successive profiles includes bearing performance, surface variations and the repeatability of the measuring process. These results therefore represent a conservative estimate of the bearing performance within the bandwidth of the measurement process.

Fig. 7: Slideway showing the layout of the UHMWPE bearings (slideway shown upside down).

The stylus probe utilized two beryllium copper cantilevers in a parallelogram type flexure that applied a constant force of less than 50 mN and had a spherical sapphire contact probe tip diameter of 2 mm, which also served as a mechanical filter to attenuate measurements of surface finish of the specimen. An in-house designed capacitance gage was used to measure the vertical displacement of the stylus. The capacitance gage based stylus was calibrated by the use of a 0.8 μm step height, which provided a sensitivity of 256 $nm \cdot V^{-1}$ with a subsequent recalibration after 6 months producing a sensitivity within 2% of the original calibration. Noise of the stylus profilometer was measured to be approximately 1.5 nm with a 0.2 nm

rms value. It is believed that the source of noise is mainly contributed by the lock-in amplifier's ability to measure a voltage change of the capacitance gage.

6. Test Results

6.1. Pin-on-Disk in Air

The pin-on-disk instrument was utilized to measure the friction coefficient and wear of the first and second bearing designs. Prior to testing the bearings and counterface surfaces were cleaned by applying alcohol using a cotton swab. No further treatments were applied throughout each test. The glass counterface was a pure silica disk polished to an optical quality with a surface roughness of better than 10 nm and flatness better than $\lambda/4$.

Table 2: Dynamic friction coefficient of 2.38 mm radius bearing (first prototype) at various speeds.

Direction	Load (N)	Speed ($mm \cdot s^{-1}$)	Dynamic Friction Coefficient	Comments
Forward	2.2	4.2	0.19	Bearings show no appreciable wear characteristics. Contact area shows little to no effect of sliding after a short run-in period.
		8.3	0.19	
	4.4	4.2	0.18	
		8.3	0.18	
	6.6	4.2	0.16	
		8.3	0.16	
	11.5	4.2	0.19	Bearing failed after approx. 700 meter traverse
		8.3	na	
Reverse	2.2	4.2	0.19	Bearings show no appreciable wear characteristics. Contact area shows little to no effect of sliding after a short run-in period.
		8.3	0.19	
	4.4	4.2	0.18	
		8.3	0.18	
	6.6	4.2	0.16	
		8.3	0.16	
	11.5	4.2	0.19	Bearing failed after approx. 700 meter traverse
		8.3	na	

Friction coefficients were measured as the average deviation from the zero frictional load measured over multiple revolutions of the disk. Average friction coefficients of the

first bearing prototype were between 0.16 and 0.19 at various normal loads and surface speeds as shown in Table 2. As might be expected, similar values were measured with the disk rotating in 'forward' and 'reverse' directions. With the exception of the highest loads at which failure occurred, the friction coefficient decreased as the load increased further supporting the theoretical prediction of an increase in friction force and a decrease in friction coefficient (μ) as the load is increased.

Table 3: Dynamic friction coefficient of 6.35 mm radius bearing (second prototype) at various speeds.

Direction	Load (N)	Speed ($mm \cdot s^{-1}$)	Dynamic Friction Coefficient	Comments
Forward	2.2	4.2	0.19	Bearings show no appreciable wear characteristics. Contact area shows little to no effect of sliding after a short run-in period.
	4.4	4.2	0.17	
	6.6	4.2	0.15	
	11.5	4.2	0.14	
	16.5	4.2	0.13	
	27.8	4.2	saturated	Outside sensors range
Reverse	2.2	4.2	0.19	Bearings show no appreciable wear characteristics. Contact area shows little to no effect of sliding after a short run-in period.
	4.4	4.2	0.17	
	6.6	4.2	0.15	
	11.5	4.2	0.14	
	16.5	4.2	0.13	
	27.8	4.2	saturated	Outside sensors range

The first prototype bearing (2.38 mm radius) catastrophically failed at a normal load of 11.5 N and a velocity of 4.2 $mm \cdot s^{-1}$ after a traverse of approximately 700 m. The second prototype brearing (6.35 mm radius) described earlier had an experimental friction coefficient between 0.13 and 0.19, noting again, that as the load increases, the friction coefficient decreases. Table 3 shows the test results of the second prototype bearing. Fig. 8(a) shows data collected of the second generation of a short-term test with three reversals of direction. The periodicity in the friction force corresponds to the complete rotation of the disk. Features of the frictional force with each rotation were found to be within 1 percent of

successive rotations. Durability of the bearing design was assessed with a long-term constant velocity experiment continually running over a 145 hour period. Fig. 8(b) shows a trial run of 45 hours with an approximate 28 N normal load and a surface speed of 4.2 $mm \cdot s^{-1}$. No significant performance change of the bearing and/or counterface was observed after approximately 2.2 km of travel.

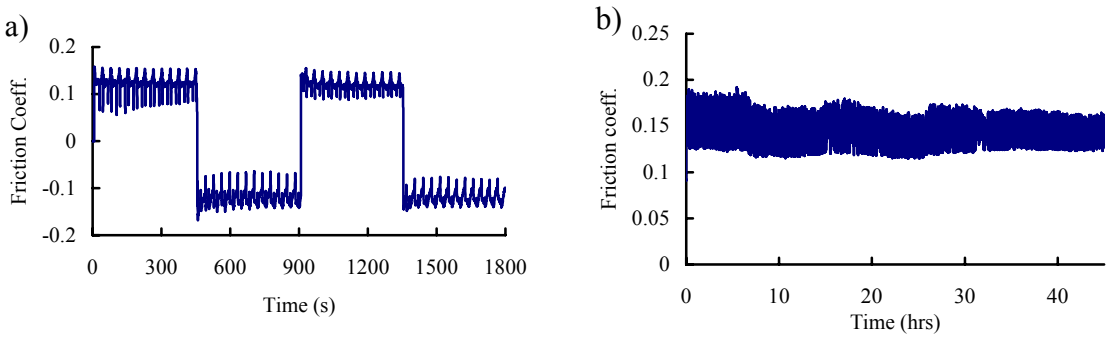

Fig. 8: a) Friction coefficient as a function of time for the 2nd generation bearing under an 11.45 N load. Data includes three changes in direction. b) Friction coefficient as a function of time for a 6.65 N normal load over a 45 hour period.

6.2. Pin-on-Disk in Vacuum

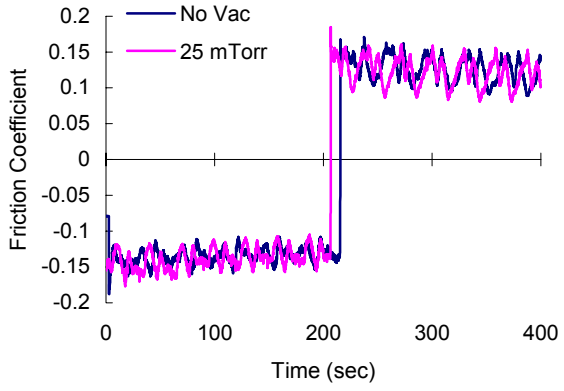

Fig. 9: Comparison between friction coefficient observed in air and vacuum (25 mTorr).

Performance evaluation of this second bearing design (UHMWPE was replaced after testing the bearing in air) was repeated in a low vacuum environment of approximately 3.3 Pa. Fig. 9 shows a comparison between measurements taking in air and at moderate vacuum (~ 3.3 Pa) with little to no deviation in friction coefficient observed. Testing for wear of the bearing resulted in a traverse of over 2.3 km at a

maximum normal load of approximately 28 N and a surface speed of 4.2 $mm \cdot s^{-1}$ (total traverse is the sum of the distance traveled for all experimental friction coefficient tests) without any significant performance changes. It should be noted that the bearing was removed from the pin-on-disk instrument at about 1.6 km to inspect the condition of the bearing. After inspection the bearing was mounted back into the instrument nominally within its original orientation. This low wear rate of the second prototype bearing in linear sliding contact has been speculated by others to be caused by the preferred orientation of surface molecules and irreversible work leading to a strain hardening of the polymer [15].

6.3. Stylus Profilometer

A capacitance based stylus profilometer described earlier was used to determine the off-axis motion repeatability of the UHMWPE bearing stage in sliding contact with an optically polished Zerodur® flat. This flat had a surface roughness of better than 10 nm and a flatness of better than $\lambda/4$. LabVIEW™ was used to collect the stylus output and laser interferometer carriage position data. Tilt was removed from the raw data using a linear curve fit resulting in the residual motion of the stage during a translation. The stage was cycled back and forth over a 10 mm traverse range. Fig. 10 illustrates the residual motion of the stage with the tilt removed over three full cycles. This profile showed an amplitude of less than 10 nm and a repeatability of the bearing to within a few nanometers. It should be noted the difference between the two profiles are due to the action of the micrometer on the carriage as well as the stylus being subject to opposing frictional forces when moving in each direction. Generally, when the slideway is pulled, the frictional forces provide a self-correcting moment. It is believed that the periodic variation observed when the carriage is pushed is the run-out of the micrometer spindle that will vary periodically with the pitch of

the micrometer, transmitting through the decoupling mechanism. This results in a clearly visible periodic variation of approximately 10 nm of the carriage. This is significantly attenuated when the carriage is pulled. Even so, this variation does not affect the performance of the bearing as the repeatability of successive profiles still falls within a few nanometers. Furthermore, the performance of the bearing is considered to be better than the estimate, based on the data of Fig. 10 since it is unlikely that the stylus will traverse the same path of the specimen thereby adding a further source of uncertainty. Notwithstanding these sources of uncertainty, it is apparent that profile features of less than a few nanometers are being resolved in successive traversals thereby indicating that the mechanical noise of the bearings is at nanometer or even sub-nanometer levels and therefore comparable to noise measured with PTFE bearings [16].

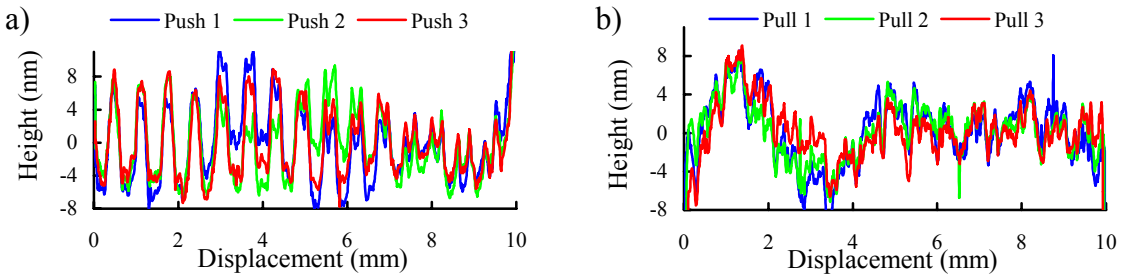

Fig. 10: Residual motion of the rectilinear slide as it is being pushed and pulled by the stage drive mechanism.

7. Acknowledgements

The authors would like to thank Lei Dong and Gregory Caskey (UNC-Charlotte) for their contribution towards this project and Dr. Vivek Badami for supplying an optically finished silica disk. We are also thankful to the University of North Carolina at Charlotte's

Center for Precision Metrology and the National Science Foundation (NSF DMI #0210543) for their support of this project.

This work was performed under the auspices of the U.S. Department of Energy by University of California, Lawrence Livermore National Laboratory under contract W-7405-Eng-48.

[1] Lindsey K., Smith S.T. and Robbie C.J., 1988, Sub-nanometer surface texture and profile measurement with 'Nanosurf 2', *Annals of the CIRP*, **37**, 519 - 522.

[2] Leach R.K., 2000, Traceable measurement of surface texture at the National Physical Laboratory using Nanosurf IV, *Meas. Sci. Technol.*, **11**, 1162 - 1172.

[3] Lindsey K., 1991, Tetraform grinding, *SPIE*, **1573**, 129 - 135.

[4] Smith S T, Yang H and Seugling R M, 2001, Polymer bearings for nanotechnology applications, *Proc. ASPE,* **24**, 70 - 75.

[5] Wang, Y.Q. and Li, J., 1999, Sliding wear behavior and mechanism of ultra-high molecular weight polyethylene, *Material Science and Engineering*, **A266**, 155 - 160.

[6] Dowson D., Taheri S. and Wallbridge N.C., 1987, The role of counterface imperfections in wear of polyethylene, *Wear*, **119**, 277 - 293.

[7] Ruben G.C., Blanchet T.A. and Kennedy F.E., 1993, Formation of UHMWPE polymeric transfer films on sliding glass counterfaces: early and steady-state wear studied by transmission electron microscopy, *Journal of Materials Science*, **28** (4), 1045 – 1058.

[8] Unal H., Sen U. and Mimaroglu A., 2004, Dry sliding wear characteristics of some industrial polymers against steel counterface, *Tribology International*, **37**, 727 - 732.

[9] Bhushan B., 2001, Modern tribology book, CRC Press, New York, p. 550 – 551, Vol. 1.

[10] Goodfellow Corp., 237 Lancaster Avenue, Suite 252, Devon, PA 19333-1954, USA, www.goodfellow.com

[11] Smith E.H., 1994, Mechanicals engineer's reference book, Butter Worth-Heidemann Ltd., p. 9/67, 12th Edition.

[12] Yamaguchi Y., 1990, *Tribology of plastic materials*, Elsevier Science Publishing Company, Inc., New York, NY, ISBN:0-444-87445-3.

[13] Johnson K.L., Contact Mechanics, 1985, Cambridge University Press, Cambridge CB2 2RU, UK, ISBN: 0521347963.

[14] Smith S.T. and Chetwynd D.G., 1992, *Foundation of ultraprecision mechanism design*, Gordon and Breach Science Publishers, London, p. 133, ISBN: 2-88449-001-9.

[15] Wang A., Sun D.C., Yau B.E., Sokol M., Esner A., Polineni V.K., Stark C. and Dumbleton, J.H., 1997, Orientation softening in the deformation and wear of ultra-high molecular weight polyethylene, *Wear*, **203 - 204**, 230 - 241.

[16] Smith S.T., Harb S. and Chetwynd D.G., 1992, Tribological properties of polymeric bearings at the nanometer level, *J. Phys. D.*, **25** (1A), 240-248.